

General Disclaimer

One or more of the Following Statements may affect this Document

- This document has been reproduced from the best copy furnished by the organizational source. It is being released in the interest of making available as much information as possible.
- This document may contain data, which exceeds the sheet parameters. It was furnished in this condition by the organizational source and is the best copy available.
- This document may contain tone-on-tone or color graphs, charts and/or pictures, which have been reproduced in black and white.
- This document is paginated as submitted by the original source.
- Portions of this document are not fully legible due to the historical nature of some of the material. However, it is the best reproduction available from the original submission.

APPLICATION OF DIFFERENTIAL GAME THEORY
TO ROLE-DETERMINATION IN AERIAL COMBAT

A. W. Merz
Aerophysics Research Corporation

(NASA-CR-137713) APPLICATION OF N75-28822
DIFFERENTIAL GAME THEORY TO
ROLE-DETERMINATION IN AERIAL COMBAT
(Aerophysics Research Corp., Bellevue, Wash.) 57 p HC \$4.25
CSCI 12E G3/66 31028
Unclas



NATIONAL AERONAUTICS AND SPACE ADMINISTRATION
AMES RESEARCH CENTER
MOFFETT FIELD, CALIFORNIA 94035



REPLY TO: NAS 2-8844
ATTN OF: AT:241-12

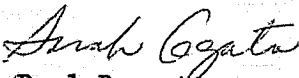
August 5, 1975

NASA Representative
Scientific & Technical Information Facility
P.O. Box 8757
Baltimore/Washington International Airport,
Maryland 21240

Subject: Transmittal of Contractor Report: "Application of Differential Game Theory to Role-Determination in Aerial Combat," by A. W. Merz, Aerophysics Research Corporation, Bellevue, Washington.

Reference: Program Code 791-40-04-01-00

The subject report prepared under Contract NAS 2-8844 has been reviewed at Ames and is recommended for release in STAR as CR-137713.

for 
Paul Bennett
Chief, Technical Information Division

Enclosure:
1 Cy Subject Report

cc:
NASA Hqrs., Code KSI (w/o encs.)

**Application of Differential Game Theory to
Role-Determination in Aerial Combat**

JULY 1975

Developed under
CONTRACT No. NAS 2-8844

A. W. Merz

Prepared by
AEROPHYSICS RESEARCH CORPORATION
Bellevue, Wash. 98009

FOR THE NATIONAL AERONAUTICS AND SPACE ADMINISTRATION
Ames Research Center, Moffett Field, California 94035

PREFACE

This report describes the theory and preliminary results of a research study carried out in the period from April to July, 1975, under Contract NAS 2-8844, titled "Study of RPV and MX System Characteristics."

Mr. Michael Tauber was the Technical Monitor for the study, which was done for the Advanced Concepts Branch of the Aeronautics Division, NASA-Ames Research Center. The author thanks Dr. J. V. Breakwell of Stanford University for providing helpful suggestions used in Sections 4.2.5 and 4.2.6. Mr. D. S. Hague of Aerophysics Research Corporation served as Project Leader for the study.

TABLE OF CONTENTS

	<u>Page</u>
1. Summary	1
2. Introduction	3
3. Mathematical Modelling	5
3.1 Methods of Developing Tactics	6
3.2 Assumptions in Mathematical Model	7
3.3 Equations of Relative Motion.	10
4. Pursuit-Evasion Maneuver Determination.	13
4.1 Terminal Conditions	13
4.2 Optimization Criteria and Necessary Conditions.	15
4.2.1 Adjoint Equations and Optimal Maneuvers.	18
4.2.2 End Conditions	20
4.2.3 Switch Conditions.	27
4.2.4 Singular Arc Conditions.	32
4.2.5 Switch Conjugate Test Condition.	34
4.2.6 An Additional Necessary Condition.	37
5. Numerical Examples of Role-Determination.	39
5.1 Heading-Limited End Condition	40
5.2 Range-Limited End Condition	44
6. Application and Generalization of Results	48
6.1 New Tactical Maneuver Rules	48
6.2 Preliminary Design of Combat Aircraft	49
6.3 Verification of Results by Computer Simulation.	50
6.4 Other End Conditions and Dynamic Models	51
7. References.	53

LIST OF FIGURES

	<u>Page</u>
Figure 2.1 Role Reversal in Aerial Combat	3
Figure 3.1 Relative Motion Coordinates.	11
Figure 4.1 Heading-Limited Terminal Conditions in A's Axis System	14
Figure 4.2 Range-Limited Terminal Conditions in A's Axis System	16
Figure 4.3 Conceptual Division of State Space	17
Figure 4.4 Terminal Trajectories on the Barrier for the Tail-Chase End Condition	21
Figure 4.5 Near Miss Trajectories	23
Figure 4.6 Near Miss Trajectory, $H_f = H_A$	24
Figure 4.7 Collision Following Maneuvers $A_R B_R$	26
Figure 4.8 Scale Drawing of Singular Arc for $V_B = .9$, $\omega_{B_{max}} = 1.5$, $H_B = 40^\circ$	33
Figure 4.9 Switch Conjugate Test (2-Dimensional)	35
Table I. Optimal Pursuit-Evasion Terminal Maneuvers (Heading-Limited End Condition)	28

APPLICATION OF DIFFERENTIAL GAME THEORY
TO ROLE-DETERMINATION IN AERIAL COMBAT

by A. W. Merz
Aerophysics Research Corporation

1.0 SUMMARY

This report describes the application of the theory of differential games to the one-on-one aerial combat problem. The purpose of the study is the development of criteria which specify the roles of pursuer and evader as functions of the relative geometry and of the important parameters of the problem.

A reduced-order model of the relative motion is derived and discussed. In this model, the two aircraft move in the same plane at unequal but constant speeds, and with different maximum turn rates. The equations of relative motion are of third order, the dependent variables being the relative range, bearing and heading of the two aircraft. Termination of the pursuit-evasion game is defined by either the heading-limited or the range-limited end condition. These are geometric conditions for which the evading aircraft is in front of the other, with the relative heading and relative range satisfying certain inequalities.

Retrograde solutions to the equations of relative motion are used with the derived optimal terminal maneuvers to find where an assumed set of end conditions could have begun. End conditions correspond to a near miss or to a collision, these being types of trajectories which define the "barrier". The barrier separates relative geometric conditions leading to capture from nearby relative conditions leading to escape, and its determination is of primary importance in the role-determination problem. It is shown that optimal maneuvers of both pursuer and evader take place at either maximum turn rate or at zero turn rate, and that the solution typically involves two-part and three-part maneuvers for both aircraft.

In general, the barriers divide the state space of relative initial conditions into three regions; namely:

1. Victory is guaranteed for aircraft A, regardless of maneuvers by aircraft B.
2. Victory is guaranteed for aircraft B, regardless of maneuvers by aircraft A.
3. Neither can win; i.e., a draw region exists in the space of initial conditions.

The contents of this report are limited to a description of the theory and an illustration of representative results obtained for typical numerical sets of parameters. The general problem is highly nonlinear, and is expected to show a strong dependence on the values assumed for the parameters. Later studies will explore this dependence, in an effort to quantify the relative importance of the various features of the problem.

2.0 INTRODUCTION

A fundamental question in the one-on-one aerial combat problem is the specification of roles. That is, which aircraft should pursue and which should evade? The answer obviously depends not only upon the relative geometry but also upon the capabilities of the aircraft and their weapon systems. From the point of view of differential game theory, these parameters alone should imply the roles and the eventual outcome of an optimally-played pursuit-evasion game. However, actual and simulated combat engagements frequently start in a configuration for which both pilots initially take the role of pursuer. One, and sometimes both of them may later switch to an evasive strategy, unless the encounter leads to a "stand-off" condition. Such a stand-off condition could arise when two equal aircraft are diametrically opposite each other, describing their minimum turn circles in the same direction.

On the other hand, the roles of pursuer and evader are obvious in those geometric configurations not far removed from an assumed end condition. Subtle changes in the initial geometry, however, can make the specification of roles less transparent, and eventually a configuration is reached for which the roles are obviously the reverse of the initial set, as shown in Figure 2.1.

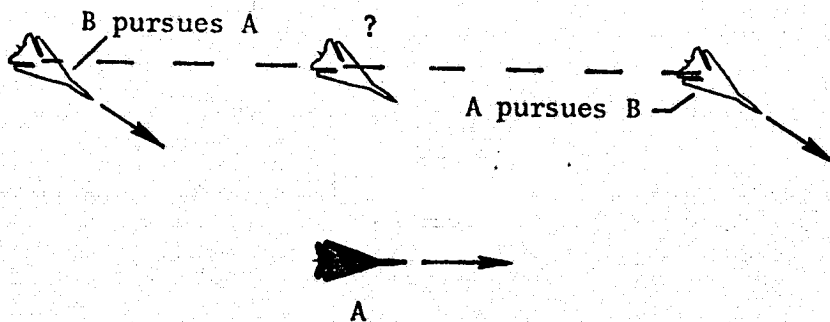


Figure 2.1 Role Reversal in Aerial Combat

The more general problem is one for which no straightforward intuitive solution exists, and which is important for the following reasons:

1. Optimal maneuver tactics are of great significance to combat aircraft pilots, whether they are pursuing or evading.
2. Relative capabilities of combat aircraft can be found in terms of speed, maneuverability and weapon systems.
3. It may be feasible to incorporate optimal combat tactics into the requirements of RPV autopilots and sensors.
4. The sensitivity of combat roles and maneuvers to certain performance parameters may be very great, such that much greater effort should be expended on these parameters; e.g., maximum turn rate at the expense of vehicle weight.

In this report, the one-on-one combat problem is mathematically modelled as a differential game^[1], in which the pursuit-evasion roles are not given a priori^[2]. The important performance parameters are constant for both aircraft and the relative position and heading are assumed known by both pilots. The parameters effectively define position in a set of "capture regions" for each of the aircraft. These capture regions are combinations of relative position (range and cone-angle) and relative heading (or angle off) for which the roles are given, and for which the pursuer is guaranteed a win, no matter what maneuvers are used by the other aircraft. A solution procedure for determining the capture region boundaries will be developed in subsequent sections of this report.

3.0 MATHEMATICAL MODELLING

Mathematical analysis of an aerial combat encounter between two aircraft is an extremely difficult problem, which can be approached in two ways:

1. Complex and accurate aircraft simulations can be used with actual or simulated pilot control inputs, to generate experimental and statistical results as to "effective" combinations of aircraft, weapon systems and pursuit-evasion maneuvers [3-10].
2. Simplified models of aircraft dynamics can be coupled with the theory of differential games to specify the roles as functions of the relative geometry and the optimal maneuvers associated with these roles.

These two methods focus on different features of the problem, and both have advantages and shortcomings. The research effort to date has been concentrated on the first approach* and a large amount of experimental data has been accumulated. However, it is difficult to draw general conclusions from the data, because of the large number of independent input parameters. Further, the experimental data may deal with a specialized feature of the problem (e.g., a gunsight or thrust-vector control system) without first showing how important this aspect is to the problem solution. However, in any case, the experimental results may be biased by the use of non-optimal control laws. This tends to make suspect any general conclusions based on experiment.

* A third method, which yields locally optimal solutions, applies the optimization criteria to the full equations of motion, over a given time-interval [11,12]. This method required that the range rate always be negative, which meant that solutions could not be found for all initial conditions.

On the other hand, practically all the published theoretical differential game studies have utilized over-simplified or over-specialized mathematical models^[13-18] or have dealt with theoretical aspects of differential games^[19,20] which are irrelevant to realistic pursuit-evasion problems.

For these reasons, it appears that detailed modelling and subsequent analysis of a portion of the aerial combat system should be done only after it has been shown to have a major impact on the system outcome. This can be demonstrated only by using simplified dynamic models which include what seem to be the fundamental features of the system.

3.1 METHODS OF DEVELOPING TACTICS

The first approach given above has the advantage of permitting practical results to be passed from experienced combat pilots to other pilots and to aircraft designers. Unfortunately, however, the mass of data accumulated in this experimental approach discourages general quantitative conclusions, and it is often impossible to know why a particular combat encounter (simulated or otherwise) ended in favor of one pilot instead of the other. Furthermore, the method is both inefficient and expensive, partly because most of the effects being simulated are secondary to the question of determining which pilot should pursue and which should evade.

The second approach, on the other hand, can be criticized as being too highly idealized with insufficient fidelity in the aircraft maneuver dynamics, and with too little attention given to the transient behavior of the pilots. Nevertheless, the analysis of reduced-order systems in the past has had the effect of isolating the significant parameters, and of permitting a more organized development of improvements in a given system. For this reason, it

is felt that practical low-order versions of the aerial combat problem can be analyzed and solved, in terms of parameters which appear to be of fundamental importance.

In order to validate or to determine limits to this hypothesis, it will be necessary to use results obtained from the simplified model in a realistic simulation of the aerial combat problem. For example, a simulated combat engagement between an "optimally" guided RPV and a comparable aircraft flown by an experienced pilot or guided by approximate combat control laws can demonstrate the value or limitations of the second approach.

3.2 ASSUMPTIONS IN MATHEMATICAL MODEL

All engineering work is based on the analysis of more or less idealized equations describing a certain aspect of the system of interest. If the mathematical details of the study are done correctly, the success and validity of such analyses depend on how well the actual system corresponds to the idealized system. For example, the low-speed small-disturbance stability characteristics of aircraft can be quite accurately determined using linearized equations written for a rigid aircraft. At higher dynamic pressures, on the other hand, aeroelastic effects become significant, and the order and complexity of the equations describing the system increase considerably. But such mathematical refinements in the system equations should be undertaken only after a rather complete study of the simpler equations. In many cases, of course, the higher-ordered equations are never needed, because the aircraft is essentially rigid for practical values of the dynamic pressures.

By analogy, the modelling of the one-on-one aerial combat problem should start with the simplest realistic* dynamic equations which can be used to describe the important features of the motion. After the pursuit-evasion tactics have been found for the simplest mathematical model, refinements can be added to the descriptive equations, and small changes in the results can normally be expected. If the changes in the results are not "small", in the engineering sense of the word, certain important assumptions have been violated. In this case, either the mathematical model must be modified, or the applicability of the results must be restricted to parameters for which such changes are small. For this reason, it is always good practice to emphasize the assumptions and conditions under which a solution has been found. The reader can then judge for himself whether these conditions are reasonable.

The velocities and maximum turn rates of the two aircraft are assumed to be constant during the encounter, to avoid the use of higher-ordered equations of relative motion. This is partially justified by observing that maximum normal accelerations due to lift are usually much larger than axial accelerations due to thrust and drag, except for very high angle of attack configurations. A second justification arises in the analogous problem of developing maritime collision avoidance maneuvers. It is found^[21,22] that ship velocities in a hard turn can be reduced by 30% to 50% from their initial values. Nevertheless, the optimal ship turn maneuvers are nearly insensitive to this change in velocity, and excellent results have been obtained by using maneuvers based on the initial velocities of the ships. Of course, any results are perfectly applicable to turn maneuvers which maintain the velocity (or energy) of the aircraft. But, if the direction of a turn maneuver can be shown to be nearly independent of the

* Instantaneous changes in speed or heading require infinite accelerations, and are examples of the use of unrealistic dynamic equations [13-16].

subsequent speed loss, it is irrelevant that the speed is reduced during the turn. In other words, the fundamental purpose of the present study is the development of pursuit-evasion maneuvers, as functions of the relative position and velocity, and not to simulate the transient behavior of the aircraft during these maneuvers.

In the development of pursuit-evasion maneuvers, it will be found useful, if not necessary, to work in terms of retrograde ("backward") time. This is the time-to-go until the end of the combat engagement, which is defined geometrically, in terms of the relative position and heading of the two aircraft. When a suitably simplified model of the aerial combat problem is solved in this way^[2,19], it is usually found that the chase is brief and the trajectories rather simple. This provides retroactive justification for certain of the assumptions necessary to the solution. That is, for example, the entire combat time may be so short that the speeds cannot be appreciably altered, so that they can reasonably be considered as constants.

The important kinematic characteristics of two aircraft in combat are the vectors describing the relative position and the relative velocity. These two vectors define a plane in which the relative motion occurs, and it is intuitively clear that both aircraft should apply their control accelerations in this plane. This makes the optimal use of the accelerations that each pilot has at his disposal, and if the individual aircraft velocities are also in this plane, an initially planar dynamics problem should remain planar. In fact, experienced combat pilots do attempt to orient their lift vector in the plane of the relative position and velocity vectors. This tends to lead to the development of an encounter lying within a twisting plane in three-dimensional space.

3.3 EQUATIONS OF RELATIVE MOTION

Under the simplifying assumptions discussed above, the relative motion is described by three equations, in which the speeds and maximum turn rates are constant parameters. The coordinate system is chosen to be fixed to the faster aircraft A, and in this axis system the relative position (x,y) and the relative heading (H) of the slower aircraft B satisfy the equations

$$\begin{aligned}\dot{x} &= -\omega_A y + V_B \sin H \\ \dot{y} &= -V_A + \omega_A x + V_B \cos H \\ \dot{H} &= -\omega_A + \omega_B\end{aligned}\quad (3.1)$$

where the turn rates are bounded; i.e., $|\omega_i| \leq \omega_{i_{\max}}$, $i = A, B$.

As shown in Figure 3.1, the relative motion can be expressed in polar coordinates as well, in terms of the cone-angle (ϕ), the angle-off (θ) and the range (r). The equations of relative motion in these coordinates are:

$$\begin{aligned}\dot{r} &= V_B \cos \theta - V_A \cos \phi \\ \dot{\phi} &= -\omega_A + (V_B \sin \theta + V_A \sin \phi) / r \\ \dot{\theta} &= \omega_B - (V_B \sin \theta + V_A \sin \phi) / r\end{aligned}\quad (3.2)$$

The two sets of coordinates are related by

$$x = r \sin \phi, \quad y = r \cos \phi, \quad H = \phi + \theta. \quad (3.3)$$

The differential equations of motion in Eq. (3.1) are seen to be linear, whenever ω_A and ω_B are constant, with solutions in terms of trigonometric functions. This is because the aircraft are then describing simple circular arc paths in fixed coordinates. The equations are solved by first determining the heading as a linear function of time, and by then solving the position equations by standard methods. The more symmetrical polar equations in (3.2), however, can be solved only in terms of arc tangent functions. These equations show how the angles ϕ and θ depend upon both the aircraft turn rates and the kinematics of the problem. When the range is large, $\dot{\phi} \cong -\omega_A$ and $\dot{\theta} \cong \omega_B$, but otherwise, highly nonlinear effects can predominate. Thus, at large ranges A can control the cone angle, but B can control the angle-off! Since from symmetry the converse is true, aircraft at an initially large distance from each other will often null the steering errors and turn the initial encounter into a head-on pass with little lateral offset. However, short-range maneuvers are far more complex.

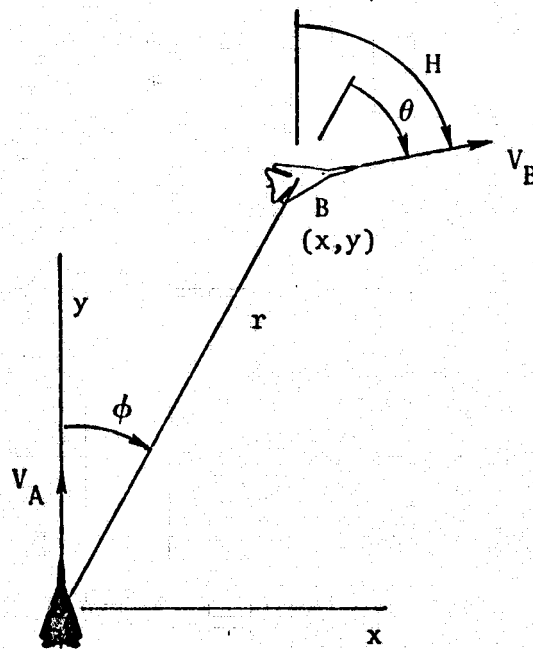


Figure 3.1 Relative Motion Coordinates

The solutions to Eq.(3.1) are given here in terms of the final (terminal) conditions (x_f, y_f, H_f) . For constant values of the two turn rates, both aircraft describe circular arcs in real space, and B's position relative to A is given by the following functions of the retrograde time, τ :

$$x = \omega_A(1 - \cos \tau + y_f \sin \tau) + V_B/\omega_B [\cos(H_f + \omega_A \tau) - \cos H]$$

$$y = y_f \cos \tau + (1 - \omega_A x_f) \sin \tau - V_B/\omega_B [\sin(H_f + \omega_A \tau) - \sin H]$$

$$H = H_f + (\omega_A - \omega_B) \tau, \quad |\omega_i| \leq \omega_{i_{\max}}, \quad i = A, B \quad (3.4)$$

Here, the velocity of the faster aircraft has been normalized to $V_A = 1$, and the maximum turn rate of this aircraft is normalized to $\omega_{A_{\max}} = 1$. This means that the unit of distance in the normalized equations is the turn radius of aircraft A. For brevity, the maximum turn rate of the slower aircraft is written as $\omega_{B_{\max}} = \omega$, which will be assumed greater than 1, while B's velocity is $V_B < 1$. The slower aircraft (B) is therefore assumed to be more maneuverable than the faster aircraft (A). This will be the case, for example, if the turns are made at the same load factor, so that the product of speed and maximum turn rate is constant for both aircraft.

4.0 PURSUIT-EVASION MANEUVER DETERMINATION

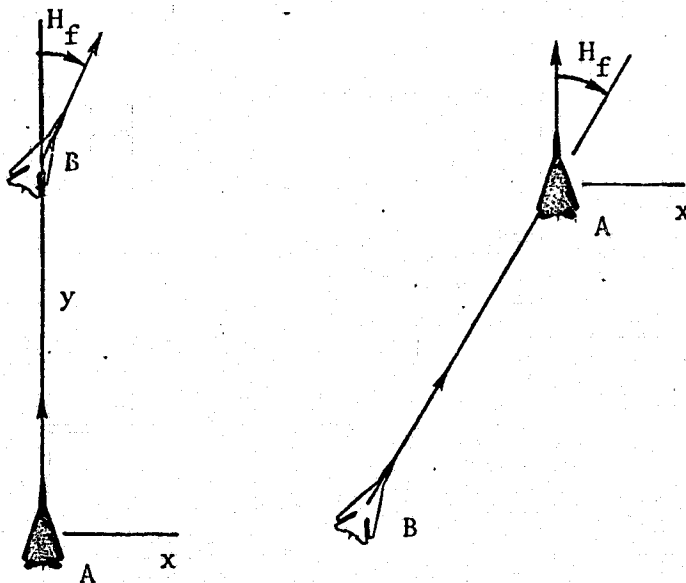
The equations of coplanar relative motion derived in the previous section provide a dynamic model of the aerial combat problem, in terms of a small number of parameters and dynamic variables. From the points of view of the aircraft pilots, the solution to the combat problem should give the roles and the maneuvers of both pilots as functions of the relative geometry. This is also the point of view taken here where, however, it is necessary to investigate the more subtle dependence of the optimal maneuvers on the aircraft velocities and maximum turn rates.

4.1 TERMINAL CONDITIONS

Termination in an aerial combat encounter can be defined in many different ways, all of which mean that the differential game has ended. A conflict exists, however, between the complex limitations of current air to air weapon systems and the requirement of relative simplicity in the mathematical models of these systems. The terminal conditions are actually functions of many independent physical quantities, but for the purposes of this report, they must be defined in much simpler terms, in order to be useful from the mathematical point of view.

Many earlier mathematical versions of the aerial combat problem^[3,13-19] have used the range alone as a termination criterion. This is a natural mathematical choice, since the capture circle (or sphere) is an extremely simple geometric shape free of the "corners" or "edges" that introduce complications when other criteria are used. This cannot be used, of course, when both aircraft can pursue, and it is necessary to specify a set of terminal conditions which are both realistic and yet simple enough to be modelled.

One physically appealing termination criterion can be described as the tail-chase or heading-limited condition, in which the evader is ahead of the pursuer, with a nearly parallel heading. This is shown in Figure 4.1 for both A pursuing B and B pursuing A. In both cases, A's velocity is aligned with the y-axis, while B's velocity is oriented at the clockwise (positive) angle, H_f .



a) A pursues, B evades

$$x_f = 0$$

$$y_f \geq 0$$

$$|H_f| \leq H_A$$

b) B pursues, A evades

$$x_f = y_f \tan H_f$$

$$y_f \leq 0$$

$$|H_f| \leq H_B$$

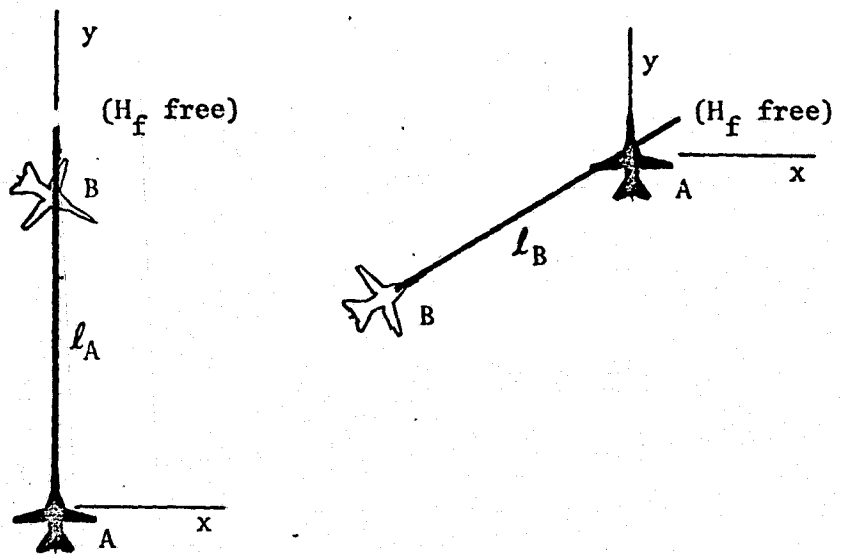
Figure 4.1 Heading-Limited Terminal Conditions
in A's Axis System

The angular parameters H_A and H_B are specified a priori, and are expected to have values of approximately 10° - 30° . These would actually depend on the details of the gun-sight or missile guidance system used by the aircraft. The range at termination can also be an important factor in the realistic modelling of the aerial combat problem, but in the heading-limited case, the final range is considered as irrelevant. This is consistent with the assumption that the forward-firing weapons of both aircraft have "long-range" guidance systems which can follow any subsequent evasive maneuvers of the target. A more detailed model of the problem would also include the final "angle-off" or bearing as a parameter; instead of requiring that the evader be exactly ahead of the pursuer at the end of the chase. In this case, too, it is felt that sufficient complexity already exists in the problem statement and that any generalization of this kind can be postponed for the present.

A second physically motivated termination criterion is defined with either airplane in front of the other, with arbitrary relative heading, but within a given range^[2]. These terminal conditions are illustrated in Figure 4.2. The range-limited case is also briefly examined in this report, and the associated maneuvers and capture regions are found for a particular numerical set of parameters.

4.2 OPTIMIZATION CRITERIA AND NECESSARY CONDITIONS

The principal results being sought in this analysis are the sets of initial conditions for which a win is guaranteed for the pursuer, regardless of the maneuvers used by the evader. The pursuer, of course, can be either aircraft A or B, and it is expected that the "capture regions" of A and B will intersect on



a) A pursues, B evades

$$x_f = 0, 0 \leq y_f \leq l_A$$

b) B pursues, A evades

$$x_f = y_f \tan H_f, r_f \leq l_B$$

Figure 4.2 Range-Limited Terminal Conditions
in A's Axis System

those surfaces which separate the two regions. That is, the state space, as described by the vector (x, y, H) , will be composed of at most three regions, corresponding to wins by A or B, and to a "stand-off" or escape by the faster aircraft. For other values of the parameters (e.g., if the faster aircraft is also more maneuverable) the third or "escape" region may be absent, and one or the other aircraft must win for all initial conditions [2].

The capture region of either aircraft is determined by a consideration of the family of "barrier"^[1] trajectories. This family of trajectories forms a "semi-permeable surface", which prevents the state from crossing the surface as long as both aircraft maneuver optimally in its neighborhood. Along the paths on this surface, the pursuit-evasion roles are known, and the trajectories end in a "near-miss" or simultaneous kill configuration.

(For the weapon models used here, a simultaneous kill is actually a collision with near-parallel headings.) The reasoning is that a small displacement normal to the barrier means a clear win or a clear escape by the pursuer or evader, respectively. Therefore, the pursuer's semi-permeable surface locally divides the state space into capture and escape regions, for the assumed roles. But, a different set of barrier trajectories exists for the reversed-role assumption and when the two barriers intersect, one or the other must be discontinued. An exception occurs on the "collision" barrier, which is itself a role-reversal locus. These notions are illustrated in Figure 4.3.

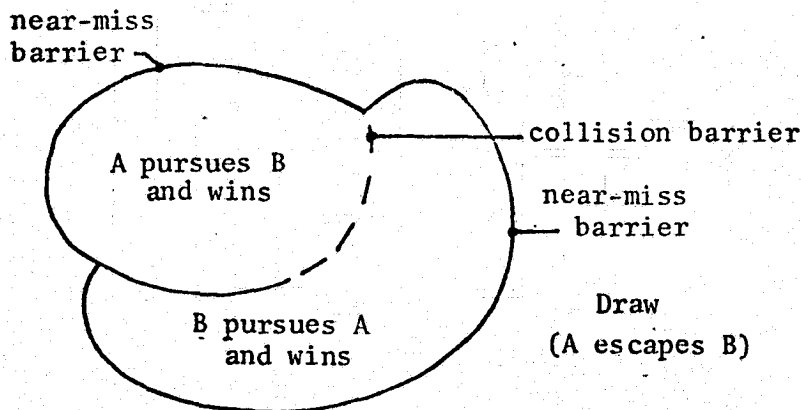


Figure 4.3 Conceptual Division of State Space

The pursuit-evasion game can be given a positive value if B wins, and a negative value if A wins, where "winning" is defined for A and B by a terminal configuration in favor of either, as shown in Figures 4.1 and 4.2. The value of the game for trajectories following the barrier is therefore zero, and this

value function has a total time derivative along the optimal trajectories which is also zero. This is the "Main Equation" of Isaacs^[1], which takes the following form,

$$\min_{\omega_A} \max_{\omega_B} [\lambda_x \dot{x} + \lambda_y \dot{y} + \lambda_H \dot{H}] = 0$$

Substituting from Eq.(3.1) with $V_A = 1$,

$$\begin{aligned} \min_{\omega_A} \max_{\omega_B} [& \lambda_x (-\omega_A y - V_B \sin H_A) \\ & + \lambda_y (-1 + \omega_A x + V_B \cos H_A) \\ & + \lambda_H (-\omega_A + \omega_B)] = 0 \end{aligned} \quad (4.1)$$

4.2.1 ADJOINT EQUATIONS AND OPTIMAL MANEUVERS

The adjoint vector, $\nabla\lambda = (\lambda_x, \lambda_y, \lambda_H)$ consists of partial derivatives of the payoff function, for which a saddle-point solution is sought. These variables obey a set of linear differential equations, which are found by differentiating Eq.(4.1) with respect to time:

$$\begin{aligned} \dot{\lambda}_x &= -\omega_A \lambda_y \\ \dot{\lambda}_y &= \omega_A \lambda_x \\ \dot{\lambda}_H &= V_B (\lambda_y \sin H - \lambda_x \cos H) \end{aligned} \quad (4.2)$$

The retrograde solutions to these equations are expressed in terms of the final values of the adjoints and the time-to-go, τ :

$$\begin{aligned}\lambda_x &= \lambda_{x_f} \cos \tau + \lambda_{y_f} \sin \omega_A \tau \\ \lambda_y &= -\lambda_{x_f} \sin \omega_A \tau + \lambda_{y_f} \cos \tau \\ \lambda_H &= \lambda_{H_f} + V_B / \omega_B [\lambda_{x_f} (\sin H_f - \sin(H_f - \omega_B \tau)) \\ &\quad + \lambda_{y_f} (\cos H_f - \cos(H_f - \omega_B \tau))] \end{aligned} \quad (4.3)$$

It will be shown that the terminal values of the adjoints are derivable from the geometric conditions at the final time, when $\tau = 0$.

The optimization procedure implied in Eq.(4.1) gives the turn-rate controls of both pilots as functions of the current values of the state and adjoint variables;

$$\omega_A = \omega_{A_{\max}} \operatorname{sgn} S_A$$

$$S_A = \lambda_x y - \lambda_y x + \lambda_H$$

and

$$\omega_B = \omega_{B_{\max}} \operatorname{sgn} S_B = \omega \operatorname{sgn} S_B \quad (4.4)$$

$$S_B = \lambda_H$$

where the switch functions of A and B are denoted S_A and S_B respectively.

The optimal maneuvers for both aircraft are therefore hard turns to left or right unless the switch function is identically zero. In this case, it can be shown that the corresponding optimal maneuver is a "dash" or straight path, for which the turn rate is zero. Thus, regardless of the relative geometry or performance characteristics of the aircraft, only nine maneuver pairs (3 maneuvers for each of 2 aircraft) are candidates for optimal controls in this model of the aerial combat problem.

4.2.2 END CONDITIONS

The optimal maneuvers can be computed only when the switch functions are known, which requires that the adjoints be known. Boundary conditions on the adjoints, however, are known only at the time of termination, when the geometry corresponds to the "near-miss" or "collision" end condition. Further analysis therefore requires consideration of the relative motion which precedes the barrier end conditions, examples of which are shown in Figures 4.1 and 4.2.

The barrier trajectories which precede these end conditions are of two general types:

1. "Near miss" trajectories for which the evader contacts tangentially the edge of the pursuer's capture region,
2. "Collision" trajectories, for which "wins" occur simultaneously for both aircraft.

These trajectories are representative solutions to the game of kind^[1], which separate "capture" from "escape", and which will be illustrated for the tail-chase end condition in the following paragraphs.

Parameters H_A and H_B were defined in Figure 4.1, and are shown in a perspective drawing of the two capture regions in Figure 4.4. These relative heading angles in the tail-chase end condition bound a two-dimensional region in the relative space on which capture must occur, and it is seen that the near-miss trajectories contact the capture regions either along the edges or tangentially along the surfaces. The collision trajectories occur at $x = y = 0$, along a line segment which is common to both capture regions.

Trajectories in this 3-space (x, y, H) are continuous curved paths obeying the equations of relative motion. That is, the relative "velocity" has components \dot{x} , \dot{y} , and \dot{H} , and the trajectories are smooth except where A or B switch turn rates.

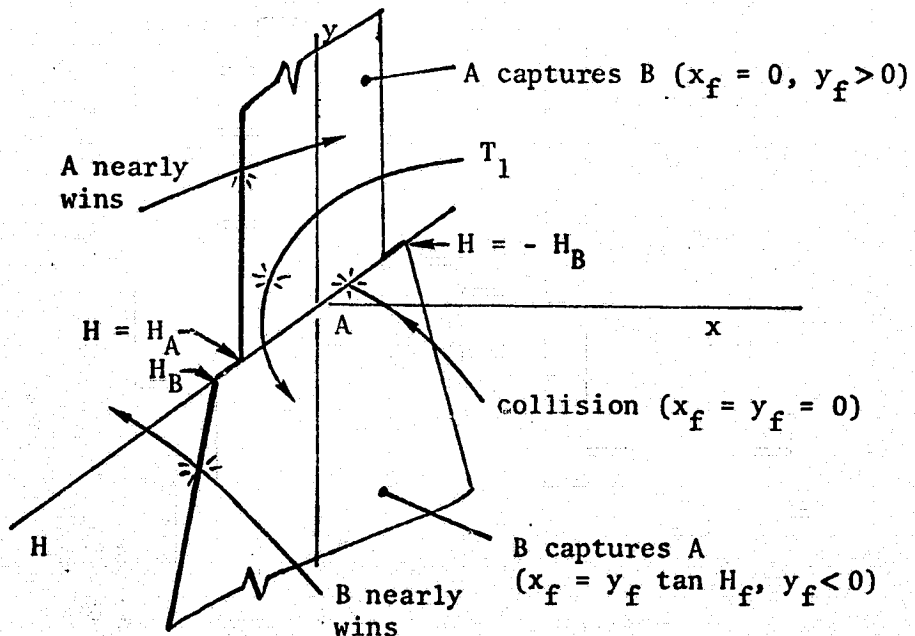


Figure 4.4 Terminal Trajectories on the Barrier for the Tail Chase End Condition

The adjoint vector $(\lambda_x, \lambda_y, \lambda_H)$ is normal to this relative velocity, according to the main equation. Consequently, a graphical interpretation can be given to this vector at the time of a near-miss or collision. The simplest such illustration is related to the trajectory "T₁" of Figure 4.4. At termination of this barrier trajectory, $\dot{x} = \dot{y} = 0$, and the adjoint vector is*

$$\nabla\lambda = (\lambda_x, \lambda_y, \lambda_H)_{t_f} = (1, 0, 0),$$

because first order changes in both y and H have no effect on the outcome of the local game. This implies that A's switch function is $S_{A_f} = \lambda_{x_f} y_f = y_f > 0$, and therefore $\omega_A = +1$ (A turns right, toward B). To determine B's terminal control, it is noted that although $S_{B_f} = \lambda_{H_f} = 0$, its retrograde derivative $(d/d\tau)$ is given by Eq.(4.2) as $\dot{S}_B = -\dot{\lambda}_H = V_B \lambda_{x_f} \cos H_f > 0$, and hence $\omega_B = +\omega$ (B also turns right, or toward the outward normal of the terminal surface). Both of these maneuvers are intuitively reasonable, and can be sketched as circular arcs in realistic space, as in Figure 4.5.

* The magnitude of the adjoint vector in a game of kind can be set equal to unity.

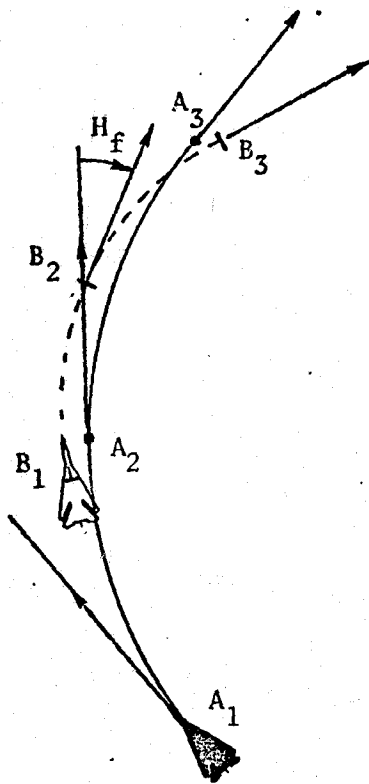


Figure 4.5 Near Miss Trajectories

The state-space locus on which these trajectories end is then found through the tangential motion condition using $\omega_A = 1$, $\dot{x}_f = -y_f + V_B \sin H_f = 0$, or $y_f = V_B \sin H_f$, where $0 \leq H_f \leq H_A$. When the near miss occurs at the limit heading, $H_f = H_A$, a more complex analysis is required to define the adjoint vector. As shown in Figure 4.6, the vector must be normal to the line $H = H_A$, $x = 0$, and it therefore has no y -component. The vector is then written as

$$\nabla\lambda = (\cos \beta, 0, \sin \beta),$$

where the angle β is obtained from the main equation; i.e.,

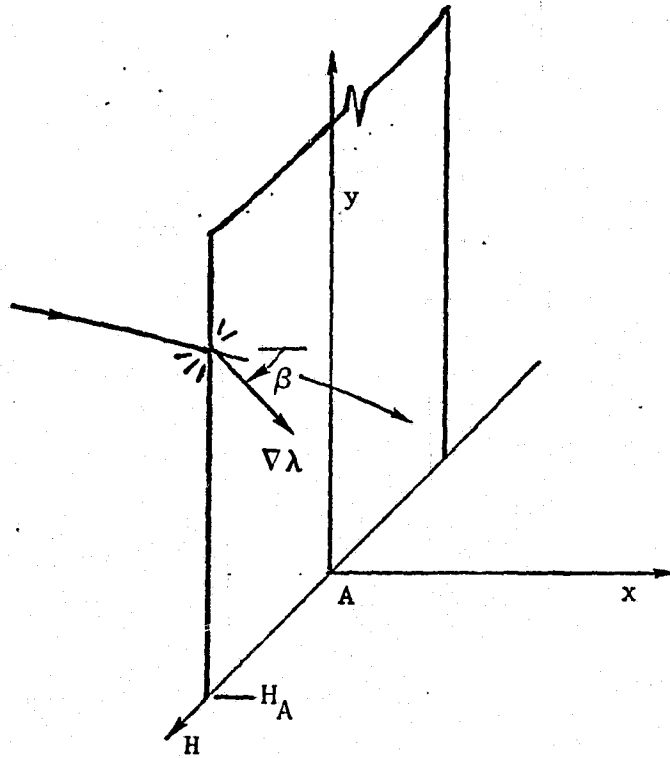


Figure 4.6 Near Miss Trajectory, $H_f = H_A$

$$\lambda_x \dot{x} + \lambda_y \dot{y} + \lambda_H \dot{H} = 0 ,$$

or

$$\tan \beta = \frac{-\omega_A y_f + \omega_B \sin H_A}{\omega_A - \omega_B} \quad (4.5)$$

Because $H_f = H_A$, B will be turning hard right in an effort to increase H_f . This means that $\sin \beta > 0$, and $\omega_B = \omega$. The turn direction of A at this time is either right or left, according to the following special subcases, which can be easily derived using Eq. (4.5).

$$\begin{aligned}
\text{a) } \omega_A &= +1 \text{ if } y_f \leq (V_B/\omega) \sin H_A, \quad \tan \beta = \frac{-y_f + V_B \sin H_A}{-\omega + 1} \\
\text{b) } \omega_A &= +1 \text{ if } y_f \geq V_B \sin H_A, \quad \tan \beta = \frac{y_f - V_B \sin H_A}{\omega - 1} \\
\text{c) } \omega_A &= -1 \text{ if } y_f \geq (V_B/\omega) \sin H_A, \quad \tan \beta = \frac{y_f + V_B \sin H_A}{-\omega - 1}
\end{aligned}$$

The collision end condition is analyzed in the same way, by assuming turn directions for A and B and then determining the terminal conditions, if any, for which such maneuvers are optimal. For example, if both are turning right at collision, the main equation is expressed with $x_f = y_f = \lambda_{H_f} = 0$, or

$$\lambda_x \dot{x} + \lambda_y \dot{y} + \lambda_H \dot{H} = \sin \beta (V_B \sin H_f) + \cos \beta (-1 + V_B \cos H_f) = 0$$

The terminal value of the angular adjoint is zero, since a first-order change in terminal heading is not to the advantage of either aircraft. Hence, the terminal adjoint vector is oriented by the angle with the tangent

$$\tan \beta = \frac{1 - V_B \cos H_f}{V_B \sin H_f} \quad (4.6)$$

The retrograde derivatives of both switch functions must be positive, since both A and B are turning right by assumption; i.e.,

$$\overset{\circ}{S}_A = \lambda_{x_f} \geq 0$$

$$\overset{\circ}{S}_B = V_B (\lambda_{x_f} \cos H_f - \lambda_{y_f} \sin H_f) \geq 0$$

Here again the superscript circle is used to abbreviate $d(\)/d\tau$.

These inequalities imply that $\sin \beta > 0$, and that

$$\lambda_{x_f} \cos H_f - \lambda_{y_f} \sin H_f = \cos H_f - V_B \geq 0$$

It is also clear on physical grounds that, since A is minimizing, $\lambda_{y_f} = \cos \beta \leq 0$, which means that $H_f \leq 0$. It is therefore concluded that A and B turn right before collision only for terminal headings in the range $-\cos^{-1} V_B \leq H_f \leq 0$ (assuming $\cos^{-1} V_B \leq H_B$). The paths in real space are sketched in Figure 4.7,

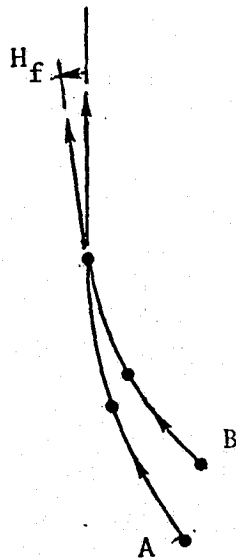


Figure 4.7 Collision Following Maneuvers $A_R B_R$

and it is seen that if either aircraft discontinues turning, it will pass ahead of the other with a relative heading less than H_B . This would mean an uncontested win for the aircraft which maintains its hard turn and, according to the problem specification, the

collision therefore represents the better of two "bad" outcomes for both aircraft A and B.

Depending on the relative orientation and turn maneuvers of the aircraft, 16 different terminal configurations are possible in this model of the problem, of which three have just been discussed. The other cases are listed in Table I, where it is seen that more stringent inequalities can occur in the applicable range of the independent variable. These inequalities can be derived by the requirement that neither switch function changes sign while the heading changes (retrogressively) from H_f to H . Further discussion of these maneuvers is postponed to Section 5.0.

4.2.3 SWITCH CONDITIONS

The retrograde integration of the state and adjoint equations allows the switch functions of both A and B to be written in terms of the terminal values of state and adjoint vectors, and the associated turn rates ω_A and ω_B . In these expressions, the independent variable is the "time-to-go" until the near miss or collision occurs. It is denoted by the symbol $\tau = t_f - t$, where t_f is the time at which the near miss or collision occurs.

By combining the results presented in Eqs. (3.4) and (4.3), the switch functions for aircraft A and B can be expressed in retrograde time as

$$\begin{aligned}
 S_A &= \lambda_{x_f} (y_f + \sin \tau) - \lambda_{y_f} [x_f - \omega_A (1 - \cos \tau)] + \lambda_{H_f} \\
 S_B &= \lambda_{H_f} + \frac{V_B}{\omega_B} [\lambda_{x_f} (\sin H_f - \sin(H_f - \omega_B \tau)) + \lambda_{y_f} (\cos H_f - \cos(H_f - \omega_B \tau))]
 \end{aligned}
 \tag{4.7}$$

where $\omega_A = \text{sgn } S_A = \pm 1$ and $\omega_B = \omega \text{sgn } S_B = \pm \omega$.

TABLE I
OPTIMAL PURSUIT-EVASION TERMINAL MANEUVERS

(Heading-Limited End Condition)

Case	Turns	Terminal State (x_f, y_f, H_f)	Terminal Adjoint ($\lambda_{x_f}, \lambda_{y_f}, \lambda_{H_f}$)
1	$A_R^B R$	$(0, 0, H_f)$ $-\cos^{-1} V_B \leq H_f \leq 0$	$(\sin \beta, \cos \beta, 0)$ $\tan \beta = \frac{1 - V_B \cos H_f}{V_B \sin H_f}$
2	$A_R^B L$	$(0, 0, H_f)$ $-H_B \leq H_f \leq -\cos^{-1} V_B$	$(\sin \beta, \cos \beta, 0)$ $\tan \beta = \frac{1 - V_B \cos H_f}{V_B \sin H_f}$
3	$A_R^B R$	$(0, V_B \sin H_f, H_f)$ $0 \leq H_f \leq H_A$	$(1, 0, 0)$
4	$A_R^B R$	$(0, y_f, H_A)$ $0 \leq y_f \leq y_{1^*}$ $V_B \sin H_A \leq y_f$	$(\cos \beta, 0, \sin \beta)$ $\tan \beta = \frac{V_B \sin H_A - y_f}{1 - \omega}$ $\tan \beta = \frac{-V_B \sin H_A + y_f}{-1 + \omega}$
5	$A_L^B R$	$(0, y_f, H_A)$ $y_{2^{**}} \leq y_f$	$(\cos \beta, 0, \sin \beta)$ $\tan \beta = \frac{y_f + V_B \sin H_A}{-1 - \omega}$
6	$A_L^B L$	$(0, 0, H_f)$ $0 \leq H_f \leq \cos^{-1} V_B$	$(\sin \beta, \cos \beta, 0)$ $\tan \beta = \frac{-1 + V_B \cos H_f}{-V_B \sin H_f}$
7	$A_L^B R$	$(0, 0, H_f)$ $\cos^{-1} V_B \leq H_f \leq H_A$	$(\sin \beta, \cos \beta, 0)$ $\tan \beta = \frac{-1 + V_B \cos H_f}{-V_B \sin H_f}$

Table I
(continued)

Case	Turns	Terminal State (x_f, y_f, H_f)	Terminal Adjoint ($\lambda_{x_f}, \lambda_{y_f}, \lambda_{H_f}$)
8	$A_L B_L$	$(0, V_B \sin H_f, H_f)$ $-H_A \leq H_f \leq 0$	$(-1, 0, 0)$
9	$A_L B_L$	$(0, y_f, -H_A)$ $y_f \leq y_1^*$ $y_f \geq V_B \sin H_A$	$(\cos \beta, 0, \sin \beta)$ $\tan \beta = \frac{V_B \sin H_A - y_f}{-1 + \omega}$ $\tan \beta = \frac{-V_B \sin H_A + y_f}{1 - \omega}$
10	$A_R B_L$	$(0, y_f, -H_A)$ $y_f \geq (V_B/\omega) \sin H_A$	$(\cos \beta, 0, \sin \beta)$ $\tan \beta = \frac{-y_f - V_B \sin H_A}{1 + \omega}$
11	$B_L A_L$	$(-\sin^2 H_f/\omega, -\sin H_f \cos H_f/\omega, H_f)$ $0 \leq H_f \leq H_B$	$(-\cos H_f, \sin H_f, -\sin H_f/\omega)$
12	$B_L A_L$	$(y_f \tan H_B, y_f, H_B)$ $-\sin H_B \cos H_B/\omega \leq y_f \leq 0$ $y_f \leq -\sin H_B \cos H_B$	$(\cos \beta \cos H_B, -\cos \beta \sin H_B, \sin \beta)$ $\tan \beta = \frac{-\sin H_B - y_f/\cos H_B}{-\omega + 1}$ $\tan \beta = \frac{\sin H_B + y_f/\cos H_B}{\omega - 1}$
13	$B_R A_L$	$(y_f \tan H_B, y_f, H_B)$ $y_f \leq -\sin H_B \cos H_B$	$(\cos \beta \cos H_B, -\cos \beta \sin H_B, \sin \beta)$ $\tan \beta = \frac{-\sin H_B - y_f/\cos H_B}{\omega + 1}$
14	$B_R A_R$	$(\sin^2 H_f/\omega, -\sin H_f \cos H_f/\omega, H_f)$ $-H_B \leq H_f \leq 0$	$(\cos H_f, -\sin H_f, -\sin H_f/\omega)$

Table I

(continued)

Case	Turns	Terminal State (x_f, y_f, H_f)	Terminal Adjoint ($\lambda_{x_f}, \lambda_{y_f}, \lambda_{H_f}$)
15	$B_R^A R$	$(-y_f \tan H_B, y_f, -H_B)$ $-\sin H_B \cos H_B / \omega \leq y_f \leq 0$ $y_f \leq -\sin H_B \cos H_B$	$(\cos \beta \cosh H_B, \cos \beta \sinh H_B, -\sin \beta)$ $\tan \beta = \frac{-\sinh H_B - y_f / \cosh H_B}{\omega - 1}$ $\tan \beta = \frac{\sinh H_B + y_f / \cosh H_B}{-\omega + 1}$
16	$B_L^A R$	$(-y_f \tan H_B, y_f, -H_B)$ $y_f \leq -\sin H_B \cos H_B$	$(\cos \beta \cosh H_B, \cos \beta \sinh H_B, -\sin \beta)$ $\tan \beta = \frac{-\sinh H_B - y_f / \cosh H_B}{-\omega - 1}$

* $y_1 = \frac{1}{\omega} [V_B \sin H_A - (\omega - 1) \sin \left(\frac{H_A - H}{\omega - 1} \right)]$

** $y_2 = \frac{1}{\omega} [V_B \sin H_A - (\omega + 1) \sin \left(\frac{H_A - H}{\omega + 1} \right)]$

For specific terminal ranges, singular arcs for both A and B can precede the maneuvers given in cases 12 and 15.

Singular arcs cannot occur just prior to termination, because this would imply

$$S_A = \lambda_x y - \lambda_y x + \lambda_H = \dot{S}_A = \dot{\lambda}_x = 0$$

or

$$S_B = \lambda_H = \dot{S}_B = V_B (\lambda_x \cos H - \lambda_y \sin H) = 0 \quad (4.8)$$

Since neither of these conditions can hold at t_f , it follows that both A and B must be turning just prior to termination of the near miss or collision maneuvers.

Because the backwards trajectories are most easily parameterized at specified (constant) values of heading, H , the solution to the heading equation (using the appropriate controls) is found as

$$H = H_f + (\omega_A - \omega_B) \tau \quad (4.9)$$

This expression gives the time-to-go, τ , when H and H_f are known, and therefore both switch functions can be calculated to assure that neither has changed sign during the retrograde trajectory of interest.

More generally, when both state and adjoints are known at t_f , the times (if any) at which S_A and S_B equal zero can be derived in terms of trigonometric arc-functions. For example, the representative case 12 from Table I can be chosen (because the less maneuverable aircraft never switches while pursuing), and for $y_f \leq -\sin H_B \cos H_B$, with both A and B turning left, the switch functions are

$$S_A = \omega (\sin H_B + y_f / \cos H_B) - (\omega - 1) \sin (H_B - \tau) . \quad (4.10)$$

$$S_B = \sin H_B + y_f / \cos H_B + V_B \left(\frac{\omega - 1}{\omega} \right) \sin \omega \tau .$$

When equated to zero, these can be solved for the retrograde-switch times,

$$\tau_A = H_B + \sin^{-1} \left[\frac{-\omega (\sin H_B + y_f / \cos H_B)}{\omega - 1} \right] \quad (4.11)$$

$$\tau_B = \frac{1}{\omega} \sin^{-1} \left[\frac{-\omega (\sin H_B + y_f / \cos H_B)}{V_B (\omega - 1)} \right]$$

Since the independent variable here is y_f , it follows that no switch occurs if the argument of the arcsin function exceeds 1 in magnitude; i.e., neither switches if the terminal range is large enough.

4.2.4 SINGULAR ARC CONDITIONS

It is possible for a singular arc to occur in the optimal path of either A or B. The necessary conditions for a singular arc in the retrograde path are that the switch function and its derivative be simultaneously zero; i.e.,

$$S_A (\tau) = \dot{S}_A (\tau) = 0$$

or

$$S_B (\tau) = \dot{S}_B (\tau) = 0 \quad (4.12)$$

As an example, we continue the study of the terminal conditions associated with case 12 of Table I, for which $x_f = y_f \tan H_B$, and $y_f \leq -\sin H_B \cos H_B$.

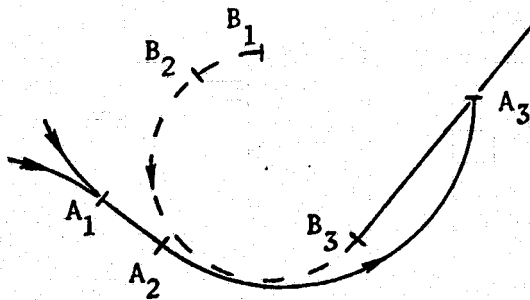
The switch functions for this terminal condition have been derived in Eq.(4.10), and the derivatives are zero at the retrograde times $\tau_A = H_B + \pi/2$, $\tau_B = \pi/2\omega$. When these times are equated to the expressions in Eq.(4.11), it is seen that a singular arc can occur for A when

$$y_f = y_{f_A} = -\cos H_B(\sin H_B + (\omega - 1)/\omega)$$

or for B when

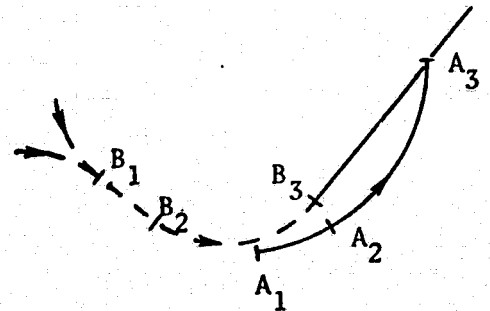
$$y_f = y_{f_B} = -\cos H_B(\sin H_B + V_B(\omega - 1)/\omega) \quad (4.13)$$

Both of these arcs can be preceded by either left or right turns, as shown in Figure 4.8. It is emphasized that these paths are only candidates for singular arcs, and that the complete solution may not include either of them.



a) Singular Arc

for A



b) Singular Arc

for B

Figure 4.8 Scale Drawings of Singular Arcs
for $V_B = .9$, $\omega_B = 1.5$, $H_B = 40^\circ$

Case 13, for which the maneuvers are $B_R A_L$, can also give rise to singular arcs. The corresponding retrograde times are

$$\tau_A = H_B + \pi/2$$

and

$$\tau_B = 3\pi/2\omega ,$$

while the terminal values of the independent position variable are

$$y_{f_A} = -\cos H_B (\sin H_B + (\omega+1)/\omega),$$

and

$$y_{f_B} = -\cos H_B (\sin H_B + V_B (\omega+1)/\omega) . \quad (4.14)$$

4.2.5 SWITCH CONJUGATE TEST CONDITIONS

When a switch occurs in a retrograde trajectory, it is necessary that the corresponding switch surface divide the state space into 2 locally separate regions. This is illustrated for a two-dimensional state in Figure 4.9. The parenthetic labels in the Figure correspond to "before" (-) and "after" (+) the switch line is encountered. In case (a), the switch conjugate condition is satisfied. In case (b), the test fails since the state space is not divided into regions corresponding to pre- and post-switching.

When the switch conjugate test is failed, it is implied that the retrograde paths cannot extend back to the switch surface, and must be interrupted by some other phenomenon or condition. This is suggested by the dashed line in Figure 4.9, which might represent a "switch envelope"^[13,18], a dispersal line^[1,2], or other condition,

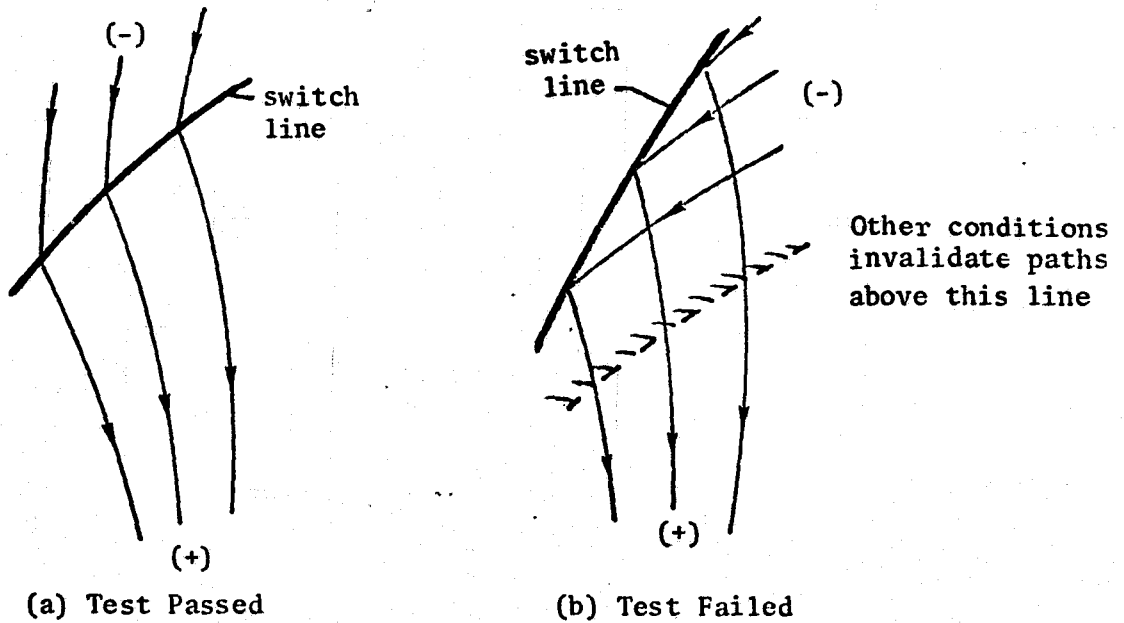


Figure 4.9 Switch Conjugate Test (2-dimensional)

derivable from other considerations. Otherwise, as noted in (b) of Figure 4.9, contradictions arise as to the controls that are optimal prior to the switch line.

For the third-order system equations describing the aerial combat problem, the switch conjugate test is more difficult to apply. The vector state is $\underline{r} = [x, y, H]$, and the switch functions have been derived as

$$S_A = \lambda_x y - \lambda_y x + \lambda_H$$

and

$$S_B = \lambda_H$$

A two-dimensional surface (e.g., $S_A = 0$ or $S_B = 0$) is described in terms of a vector normal to the surface, \hat{n} . This normal is found by calculating partial derivatives along the retrograde trajectory evaluated at the switch time.

The retrograde state is expressed for the near-miss end condition in terms of the three parameters (y_f, H_f, τ) , since $x_f = 0$ (A pursues) or $x_f = \pm y_f \tan H_f$ (B pursues). The switch time $\tau = \tau_s$ is eliminated by solving the switch functions for the time τ_s ; i.e.,

$$S_A(y_f, H_f, \tau_s) = 0 \quad \text{or} \quad S_B(y_f, H_f, \tau_s) = 0.$$

This implies a parametric expression for the two-dimensional switch surface,

$$\underline{r} = \underline{r}(y_f, H_f).$$

Now, the vector normal to the switch surface is given by the cross-product

$$\hat{n} = \underline{r}_{y_f} \times \underline{r}_{H_f},$$

where the scalar components of the normal are

$$\begin{aligned} n_x &= \frac{\partial y}{\partial y_f} \frac{\partial H}{\partial H_f} - \frac{\partial y}{\partial H_f} \frac{\partial H}{\partial y_f} \\ n_y &= \frac{\partial H}{\partial y_f} \frac{\partial x}{\partial H_f} - \frac{\partial H}{\partial H_f} \frac{\partial x}{\partial y_f} \\ n_H &= \frac{\partial x}{\partial y_f} \frac{\partial y}{\partial H_f} - \frac{\partial x}{\partial H_f} \frac{\partial y}{\partial y_f} \end{aligned}$$

The switch conjugate test then consists of an evaluation of the dot product

$$\hat{n} \cdot \underline{\dot{r}}^- = n_x \dot{x}^- + n_y \dot{y}^- + n_H \dot{H}^- ,$$

which must be positive if the vector \hat{n} is in the direction of $\underline{\dot{r}}^+$.

The test is carried out by first computing numerical values of the partial derivatives in \hat{n} , at the time τ_s . These vector components are then multiplied by the relative velocity components before (-) and after (+) the switch surface is encountered. Since τ_s implies $\underline{r}^+ = \underline{r}^-$, the velocities are different only because ω_A or ω_B has switched across the surface $S_A = 0$ or $S_B = 0$, respectively.

4.2.6 AN ADDITIONAL NECESSARY CONDITION

For near-miss maneuvers that end at $H_f = \pm H_A$ or $\pm H_B$, an additional necessary condition can be formulated. This condition should be examined because it can sometimes reject a terminal maneuver combination that might appear plausible by other considerations.

When aircraft B is pursuing, a local differential game can be defined at the time when $H_f = H_B$, and when $x_f = y_f \tan H_B$. In this near miss configuration, the relative angular heading is the payoff which B wants to minimize and A to maximize. Therefore, in this local differential game an incremental payoff is

$$\delta\lambda = \lambda_x \delta x_f + \lambda_y \delta y_f + \lambda_H \delta H_f \quad (4.15)$$

where

$$\lambda_x = \cos\beta \cos H_B, \quad \lambda_y = -\cos\beta \sin H_B, \quad \lambda_H = \sin\beta.$$

Since $\delta y_f = 0$ and $\delta x_f = y_f \delta H_f \sec^2 H_B$, the adjoint orientation angle β must satisfy

$$\frac{\delta\lambda}{\delta H_f} = \sin\beta + y_f \cos\beta / \cos H_B \leq 0. \quad (4.16)$$

On the other hand, the main equation yields the min-max condition on this angle,

$$\tan \beta = \frac{\sin H_B - \omega_A y_f / \cos H_B}{\omega_A - \omega_B} \quad (4.17)$$

where

$$\omega_A = \text{sgn}(\sin\beta + y_f \cos\beta / \cos H_B)$$

$$\omega_B = \omega \text{sgn}(\sin\beta).$$

It can be seen that that the necessary condition in Eq.(4.16) means that $\omega_A = -1$, and it is necessary to consider only the two maneuver pairs, $\omega_B = \pm\omega$. That is, if the requirement of Eq. (4.16) is not imposed on the maneuvers, the terminal controls $\omega_B = -\omega$, $\omega_A = 1$ ($B_L A_R$ in abbreviated form) are apparently optimal for $y_f \leq -\sin H_B \cos H_B / \omega$. The pair $B_R A_L$ is found to be optimal only in the range $y_f \leq -\sin H_B \cos H_B$, while $B_L A_L$ is optimal in the two negative intervals,

$$-\sin H_B \cos H_B / \omega \leq y_f \leq 0, \quad \text{and} \quad y_f \leq -\sin H_B \cos H_B.$$

5.0 NUMERICAL EXAMPLES OF ROLE-DETERMINATION

Preliminary results have been obtained for representative sets of aircraft parameters. In the examples treated, the faster aircraft, A, has a smaller maximum turn rate than aircraft B, and it is known that significant qualitative changes in the capture regions will occur if A is both faster and more maneuverable than B. It is to be emphasized that the results shown here are subject to check by results obtained at other values of the relative heading. That is, until the barrier solution has been found at all values of the relative heading (thus filling the state-space), one cannot be certain of results found at any value of the relative heading, since they may be over-ridden by conclusions found to be needed elsewhere.

Capture boundary results will now be shown graphically for each of two different definitions of capture. These definitions are:

1. The evader is directly ahead of the pursuer with the velocities nearly parallel. That is, the relative heading is within a given interval of zero and the relative range is arbitrary, at termination. This is the "heading-limited" criterion analyzed in the body of this report.
2. The evader is directly ahead of the pursuer, but within a given range, while the relative heading is arbitrary at termination. This criterion is an extension of the game studied in Ref. 2, for other values of the parameters.

The first of these is the "tail-chase" configuration illustrated in Figure 4.1, and the second end condition is illustrated for representative parameters in Figure 4.2.

5.1 HEADING-LIMITED END CONDITION

The aircraft parameters chosen for the computations are $V_B = .9, \omega_{B_{\max}} = 1.5$, while the speed and turn rate of the faster aircraft are both unity. The cone angles illustrated in Figure 4.1 are given the values $H_A = 30^\circ$ and $H_B = 40^\circ$.

Preliminary results have been found for two values of the relative heading, and these have required the use of several two-part maneuver combinations. The capture boundaries for both aircraft are shown at the relative headings of 0° and 15° in Figures 5.1(a) and 5.1(b), where the subscript notation of Section 3.2 has been used. These barrier contours are associated with all of the end conditions discussed in Section 4.2.2. It is noted that the more maneuverable aircraft B has a much larger capture region than A, because of the end condition imposed. That is, the heading variable can be controlled by B, because $\omega_B > \omega_A$, and consequently if the initial heading is outside the interval $-H_A$ to H_A , B can prevent its subsequent reduction to this interval, regardless of the maneuvers chosen by A. The results shown here indicate that a large "draw" region exists for these parameters, for which A can prevent capture by B, regardless of the maneuvers chosen by B.

Three representative real-space trajectories are shown in Figure 5.2. The initial relative geometries are indicated in Figure 5.1 as the points P_1, P_2 and P_3 . These preliminary results indicate that relatively simple approximate maneuvering rules may be devised for both pursuer and evader, but that relative heading is an important state variable in the development of these rules. More precise conclusions must await the completion of the maneuver charts for other values of the relative heading.

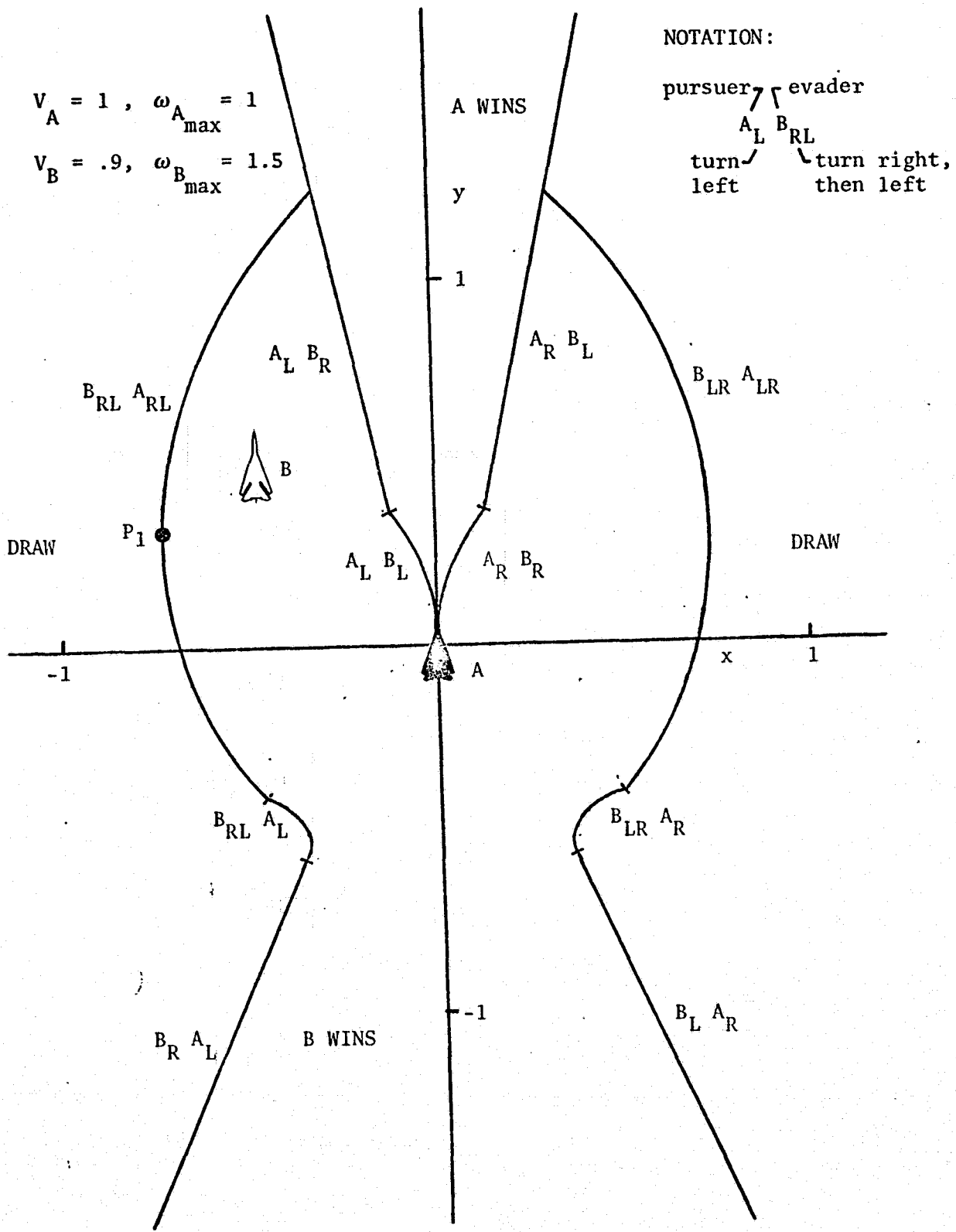


Figure 5.1(a) Tail Chase Capture Regions, $H = 0^\circ$

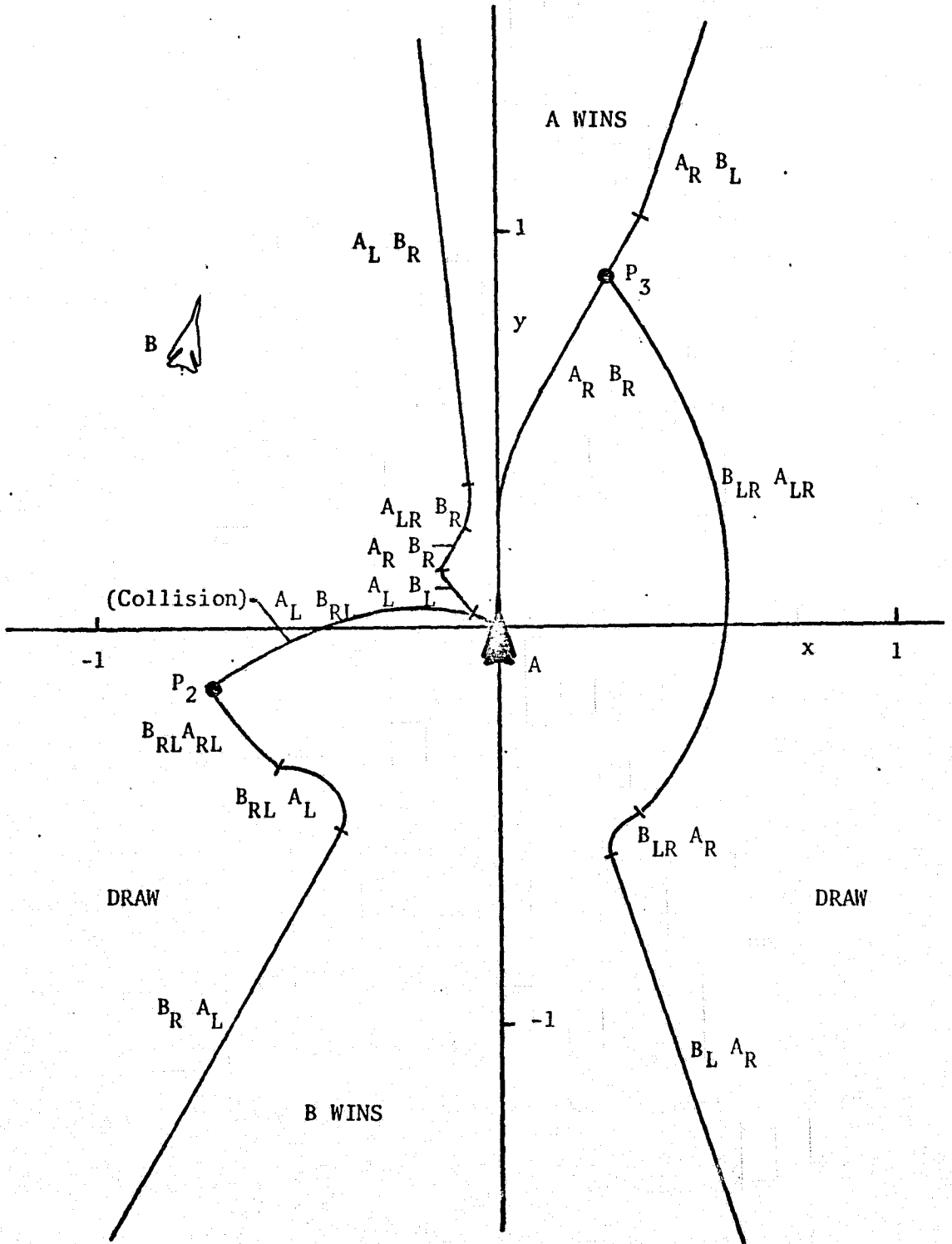
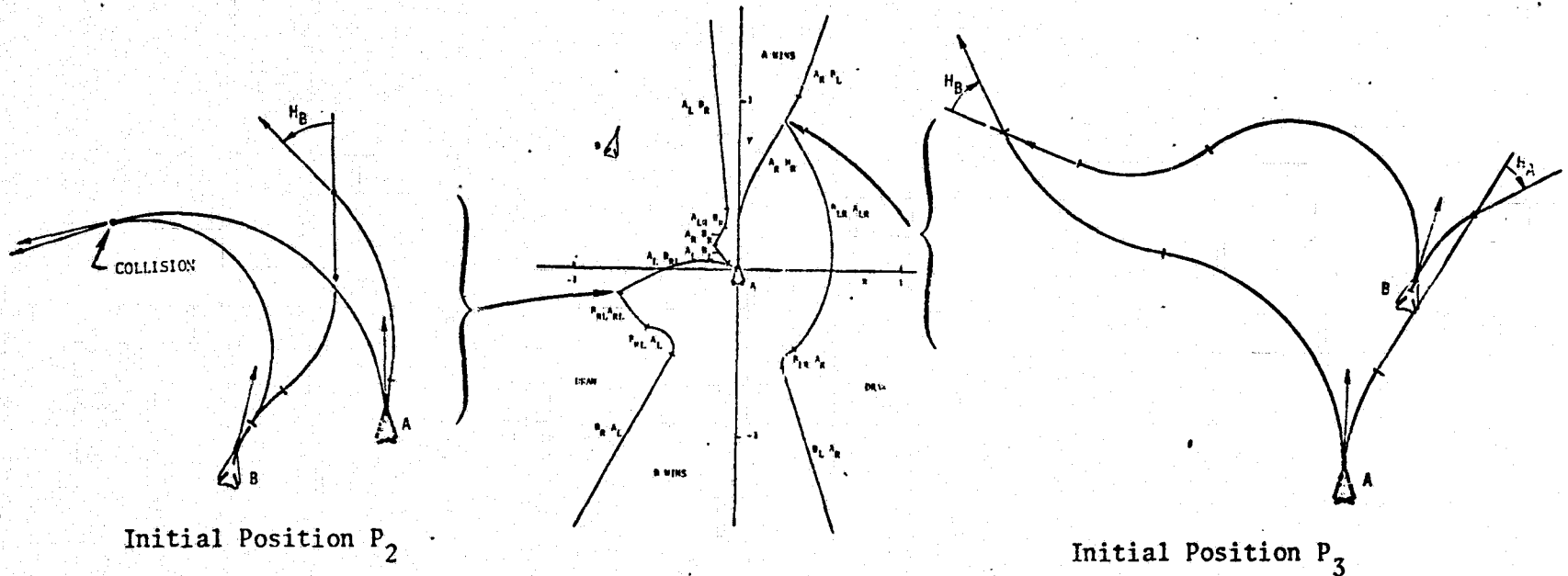
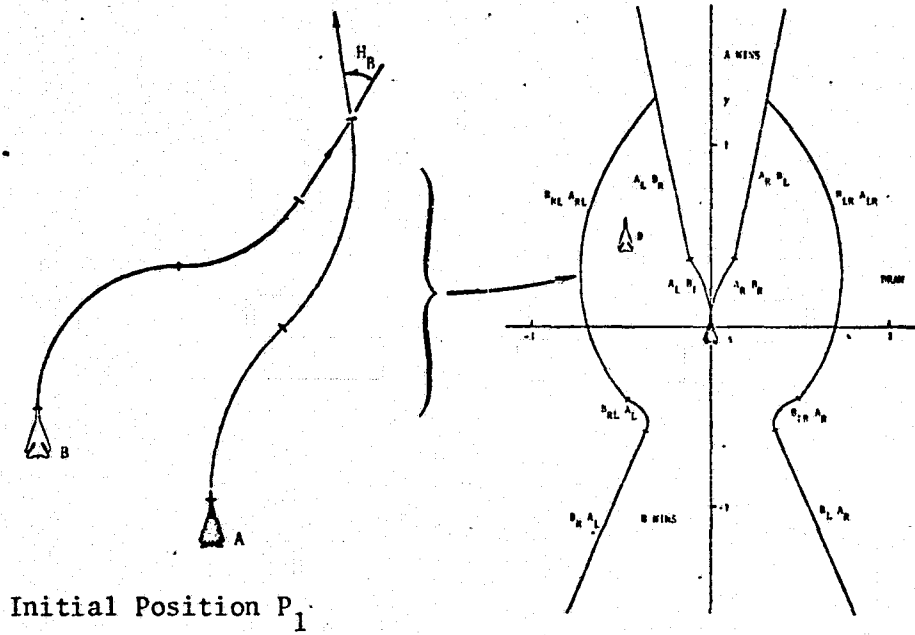


Figure 5.1(b) Tail Chase Capture Regions, $H = 15^\circ$



Initial Position P_3

Figure 5.2 Barrier Maneuvers in Real Space

5.2 RANGE-LIMITED END CONDITION

If the terminal range is bounded for both aircraft, while the terminal heading is arbitrary, with capture again occurring at zero steering error, a very different set of capture regions can be expected. In this differential game, which employs the dynamic equations of Section 3.3, the faster aircraft can always escape from the slower aircraft. This occurs, for example, if the initial range is large enough. Furthermore, in this game, the maximum turn rate is not so critical a parameter as in the heading-limited case.

Previous solutions to this game^[2] have considered different parameters, for which one aircraft had an infinite range weapon. The resulting barriers divided the state space into two regions, corresponding to A wins and B wins. In the present report, both aircraft will be constrained to finite range weapons. It will be shown that for this case three solution regions exist, corresponding to A wins, B wins, and draw.

To illustrate the capture regions in the range-limited end condition, the following parameters are chosen:

$$\begin{array}{lll} V_A = 1.0 & \omega_{A_{\max}} = 1.0 & l_A = .5 \\ V_B = .9 & \omega_{B_{\max}} = 2.0 & l_B = .6 \end{array}$$

where l_A and l_B are the weapon ranges for aircraft A and B. The computations have been developed only for the parallel-heading initial condition ($H = 0^\circ$) and the capture regions are as shown in Figure 5.3. Two marked differences are apparent between these results and those given in Figure 5.1(a) for the heading-limited end condition. These are:

1. The maneuverability of B is relatively unimportant when the terminal heading is free. In this case, the size of B's capture region depends principally on the weapon range, l_B .

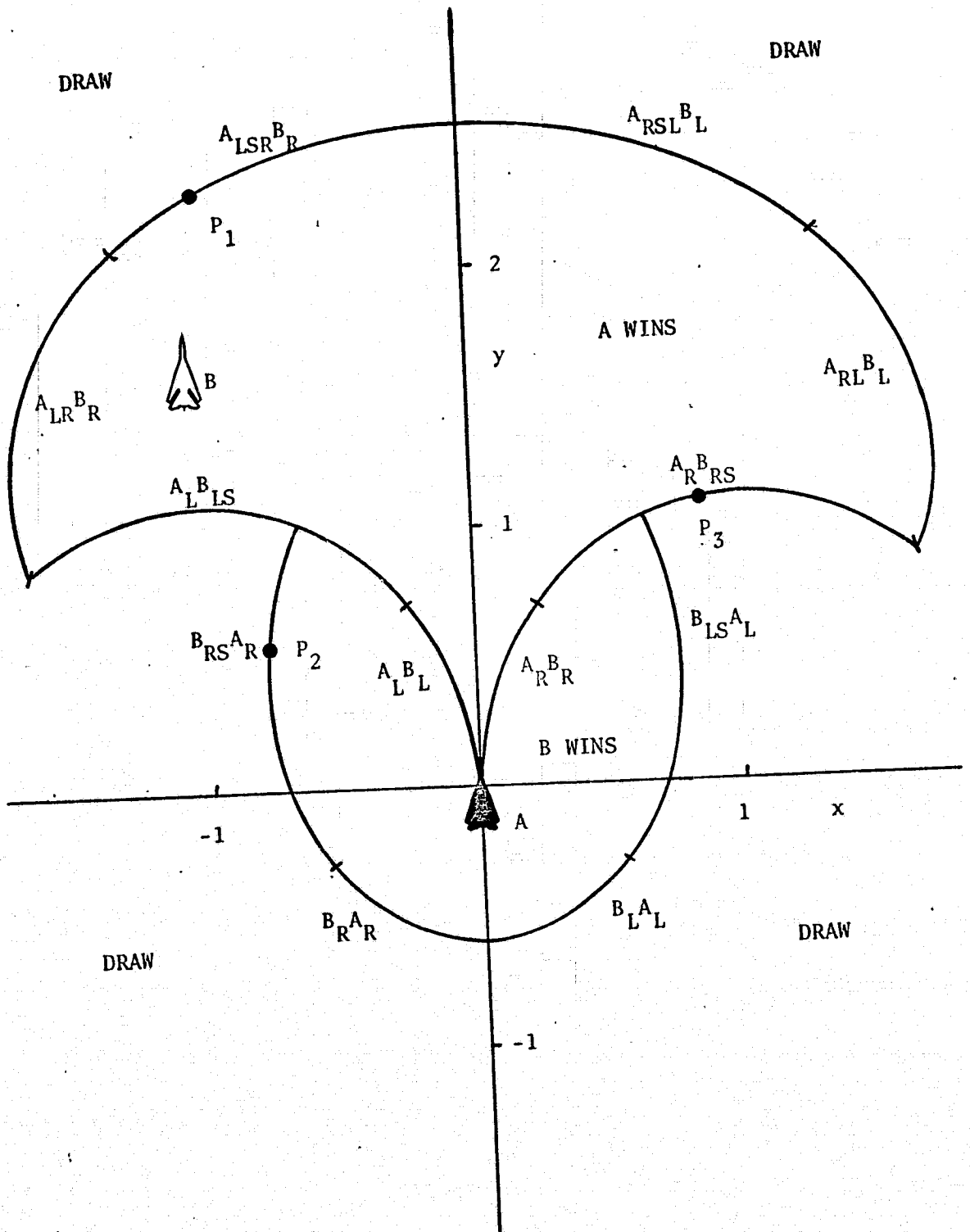


Figure 5.3 Range-Limited Capture Regions, $H_f = 0^\circ$

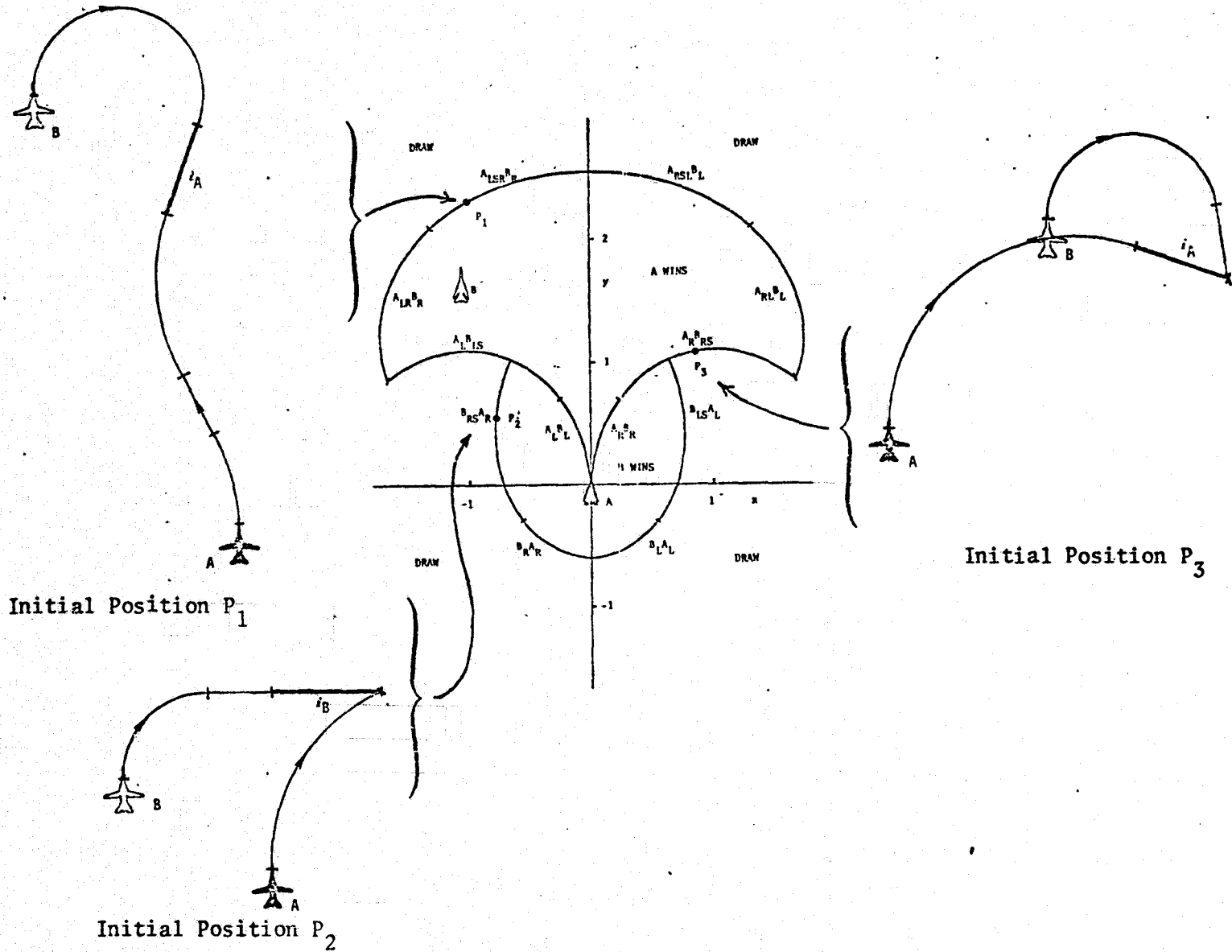


Figure 5.4 Barrier Maneuvers in Real Space

2. In the range-limited end condition, singular arcs (dashes) can occur for both aircraft. This is because, on the barrier, the maneuvers of each can be strongly influenced by the finite weapon range of the other.

Real-space trajectories of both aircraft are illustrated in Figure 5.4, corresponding to the three relative initial positions labelled P_1 , P_2 and P_3 in Figure 5.3. The forward portion of A's capture region corresponds to the simultaneous kill condition. For example, from initial position P_1 , simultaneous kill requires A to perform a three-part maneuver in response to B's simple right turn. Vehicle A's three-part maneuver (left, straight, right) precedes a head-on shot for both vehicles, which occurs at a range of $l_A < l_B$. That is, A has eluded B until B is also within range.

Other barrier segments are found for the near-miss end condition, and these can occur as either one-part or two-part maneuvers. The two cases illustrated terminate at maximum range (l_A or l_B), but near-misses can also end at shorter ranges, as shown in Figure 4.4.

The method used for displaying the solution to this problem develops loci at constant values of the relative heading. These loci are merely candidates for barrier trajectories, and they need not be continuous or part of a closed contour. That is, the various finite line segments on which the barrier paths end (Table I) correspond to other finite line segments at a given relative heading, and only the relevant portions of these line segments are shown in Figures 5.1 and 5.3. That is, for example, the point P_2 of Figure 5.1(b) marks the intersection of two segments which actually extend beyond this corner. Likewise, the barrier $B_{LS} A_L$ of Figure 5.3 is discontinued where it intersects $A_R B_{RS}$.

6.0 APPLICATION AND GENERALIZATION OF RESULTS

The dynamic model used here for the aerial combat problem includes as parameters the speeds, maximum turn rates and the required end conditions for both aircraft which can include inequality constraints on range and/or relative heading.

Even for this simplified dynamic model, extensive parametric studies are possible. Such studies would determine the capture conditions and associated maneuvers for practical ranges of speeds, turn rates, etc., with applications as described in the following subsections.

6.1 NEW TACTICAL MANEUVER RULES

When the parameters are numerically fixed, the solution to the fundamental problem of role-determination consists of the boundaries in state space corresponding to the near-miss and collision end conditions. This portion of the problem does not specify the maneuvers to be used by the aircraft when the relative state is not on these "barriers". But, capture and escape are guaranteed for initial conditions just "inside" or just "outside" of the barriers, if the pursuer and evader, respectively, maneuver optimally in the neighborhood of these barriers. This is to emphasize that:

1. Tactical maneuvers exist which guarantee a win for either aircraft, in some region (range, bearing and heading) of state space. The location of the region depends on the parameters and the definition of "win".
2. Both capture regions grow larger if the evader maneuvers non-optimally, and both decrease in size if the pursuer

so maneuvers. Nothing useful can immediately be said when both aircraft maneuver non-optimally.

3. The tactical maneuvers have been shown to be hard turns or straight dashes at all times during the combat engagement.

When the terminal geometry configuration is specified, it is conjectured that relatively simple approximate maneuver rules may be deduced from the resulting optimal solutions and trajectories. Since sharp turns represent the vast majority of the maneuvers, it is only necessary for pursuer or evader to know the direction of the turns as functions of the relative geometry.

New tactical maneuver rules are a reasonable hope for any practical model of the aerial combat problem, and certain results in this direction have already been found. For example, the turn maneuvers "right, straight, left" can occur for both aircraft, but only when the slower, more maneuverable aircraft is pursuing in the tail chase version of the problem. It is hoped that other interesting and important results of this type will be determined as the solution progresses.

6.2 PRELIMINARY DESIGN OF COMBAT AIRCRAFT

Combat aircraft can be designed competitively, if a particular enemy aircraft and weapon system are known to be of interest. For certain combat termination criteria, it is then possible to compute the capture regions of both aircraft as the performance parameters of the aircraft are varied through selected limits.

This type of analysis may show, for example, that a large increase in top speed has a very small influence on the capture volume, assuming the other aircraft parameters are constant. The costs associated with improving the propulsion or aerodynamics can then be directed to other aspects of the aircraft performance.

This type of trade-off study is impossible to perform without an understanding of the interlocking portions of the problem. While it is generally agreed that the aircraft and its guidance system (or pilot) function as a single system, the optimization of this system requires that the performance criteria be accurately defined. Although practical constraints limit the range of applicability of results which can be obtained in this way, the benefits to be obtained from such studies appear to be considerable.

6.3 VERIFICATION OF RESULTS BY COMPUTER SIMULATION

The results obtained by the methods described here can be verified and/or modified by using computer simulation methods. Such methods would replace the planar, constant speed, variable turn rate equations of motion with more complex, three-dimensional, nonlinear equations in which the maneuver transients are accurately modelled. Powerplant limitations, aerodynamic nonlinearities and control system parameters would all have some influence on these "exact equations".

The process of verification would proceed on a point-by-point basis, according to which an "approximate" point on the barrier (x, y, H) is located "exactly" by applying the approximate turn maneuvers to the exact equations of motion. As long as the ratios of speed and turn rates do not differ significantly from the values assumed in the approximate equations, the barrier contours should change only slightly from the approximate values. Such verification methods have proven highly successful in the development of collision avoidance maneuvers for ships^[21].

6.4 OTHER END CONDITIONS AND DYNAMIC MODELS

The strong dependence of the capture regions on the imposed end conditions has shown that useful results require careful definitions of "capture." The end conditions are typically expressed in terms of equalities or inequalities among the position and heading state variables in the problem.

A modification to the "tail chase" end conditions would involve the specification of a "cone-angle," or terminal bearing of the evading aircraft. This cone-angle is taken as zero in the results shown in Sec. 5.1, but a positive value for this parameter would add both to the realism and to the complexity of the computations. Bounding the terminal range for both aircraft is another obvious and important refinement in the development of the tail-chase end condition. This addition to the problem definition would have the effect of ensuring the existence of a third, "no-contest" region in the state-space, because the faster aircraft could then always escape the slower, if the initial range is large enough.

The terminal range could be given a lower limit as well, and this would have a strong influence on the shape of the capture regions. The collision trajectories, of course, would no longer occur, and the capture region for aircraft A would begin some distance ahead of A, while that of B would begin at some distance behind A, when both are shown in axes fixed to A.

Another terminal condition of practical interest involves the time interval during which the pursuer can keep the evader in the pursuer's cone-angle. The pursuer's terminal maneuvers in this case would frequently involve intermediate turn rates which have been shown to be unnecessary for the terminal conditions discussed here.

It should be emphasized again that the optimal maneuvers which have been derived and discussed thus far are associated only with the "barrier" trajectories. That is, no maneuvers are specified at arbitrary (intermediate) relative positions and headings between or outside the barriers. It is expected that maneuvers at intermediate positions could be determined by assuming a switch line at a point midway between the computed right and left barrier traces, but this is merely a rule of thumb with no theoretical justification. More formally, optimal solutions between the barriers must involve a different value function than those for the games of kind studied in this report. For example, if the capture region for aircraft A is known, the maneuvers at an interior point may be found on the basis of optimizing (in the min-max sense) the capture time. This requires the solution of the game of degree^[1,18].

The effects of changing the dynamic model will be most easily studied by first varying the constant parameters through a wide range of practical interest. If, as expected, the capture regions show a small dependence on certain of the parameters, then it is reasonable to conclude that these parameters can be approximated by constants in any practical use of the results. It may be found, for example, that while the aircraft velocities change considerably during sharp turn maneuvers^[4], these changes do not appreciably affect the location of the barrier or the associated maneuvers. Speed variations, of course, will change the time required to perform a maneuver, as was found to occur during collision-avoidance turns for ships^[22], but the maneuvers themselves may be nearly insensitive to these refinements in the dynamic model.

7.0 REFERENCES

1. R. Isaacs, Differential Games, Wiley and Sons, 1965.
2. G. J. Olsder and J. V. Breakwell, "Role-Determination in an Aerial Dogfight," International Journal of Game Theory, Vol. 3, No. 1, pp. 47-66.
3. A. L. Leatham and U. H. Lynch, "Two Numerical Methods to Solve Realistic Air-to-Air Combat Differential Games," paper 74-22, AIAA 12th Aerospace Sciences Meeting, Washington, D.C., Jan. 30, 1974.
4. D. S. Hague, R. T. Jones and C. R. Glatt, "Combat Optimization and Analysis Program, COAP," Air-to-Air Combat Analysis and Simulation Symposium, Kirtland AFB, New Mexico, February 1972.
5. T. R. Harvey and J. D. Dillow, "Application of an Optimal Control Pilot Model to Air-to-Air Combat," paper presented at IEEE Conf. on Human Operator Modelling, 1968.
6. G. H. Burgin and L. J. Fogel, "Air-to-Air Combat Tactics Synthesis and Analysis Program Based on an Adaptive Maneuvering Logic," paper presented at Air-to-Air Combat Analysis and Simulation Symposium, Kirtland Air Force Base, N.M., February 29, 1972.
7. T. K. Campbell, T. T. Gold, R. H. Andrews and W. Moore, "Application of Performance Optimization Techniques to Tactical Aircraft Operations" (U), AFFDL-TR-70-41, Vol. II, August 1970 (SECRET).
8. Anon., "Air-to-Air Combat Analysis and Simulation Symposium," (U), AFFDL-TR-72-57, Vol. I and II, May 1972 (SECRET).

9. R. L. Simpson, et al, "Weapon System Effectiveness Analysis, Optimization and Simulation - Phase I, Autopilot Parameter Optimization," Technical Report AFATL-TR-71-20, Vol. VI, February 1971.
10. D. S. Hague, "Application of Combat Simulation Techniques to Guidance Law Determination in Aerial Combat," Aerophysics Research Corporation Technical Note TN-190, July 1973.
11. D. A. Roberts, "Aerial Combat Analysis Using Differential Games," paper presented at Air-to-Air Combat Analysis and Simulation Symposium, Kirtland Air Force Base, New Mexico, February 29, 1972.
12. D. A. Roberts and R. C. Montgomery, "Development and Application of a Gradient Method for Solving Differential Games," NASA TN D-6502, 1971.
13. A. W. Merz, "The Homicidal Chauffeur," AIAA Journal, Vol. 12, No. 3, March 1974; also Stanford University, Department of Aeronautics and Astronautics Rep. 418, March 1971.
14. S. M. D. Williamson-Noble, "Singular Surfaces in Aircraft/Aircraft Differential Games, Assuming a Spherical Acceleration Vectogram for Each Aircraft," 5th Hawaii International Conference on System Sciences, 1972.
15. W. L. Othling, "Application of Differential Game Theory to Pursuit-Evasion Problems of Two Aircraft," (Dissertation) DS/MC/67-1, WPAFB, Ohio, June 1970.

16. U. H. D. Lynch, "Differential Game Barriers and Their Application in Air-to-Air Combat," (Dissertation) DS/MC/73-1, WPAFB, Ohio, March 1973.
17. W. Y. Peng and T. L. Vincent, "Some Aspects of Aerial Combat," AIAA Journal, Vol. 13, No. 1, January 1975.
18. A. W. Merz, "The Game of Two Identical Cars," Journal of Optimization Theory and Applications, Vol. 9, No. 5, May 1972.
19. W. W. Willman, "Formal Solutions for a Class of Stochastic Pursuit-Evasion Games," Technical Report No. 575, Division of Engineering and Applied Physics, Harvard University, Cambridge, Mass., November 1968.
20. Y. C. Ho, et al, Ed., "Proceedings of the First International Conference on the Theory and Applications of Differential Games," Univ. of Massachusetts, Amherst, Mass., September 29, 1969.
21. J. A. Sorensen, et al, "Final Report, Collision Avoidance System Analysis - U.S. Maritime Administration," Systems Control, Inc., Palo Alto, California, July 1975.
22. A. W. Merz and J. S. Karmarkar, "Collision Avoidance Systems and Optimal Turn Maneuvers," The Journal of Navigation, to appear.